

1 *Conference Proceedings Paper*

# 2 Use of statistical approach combined with SAR 3 polarimetric indices for surface moisture estimation 4 over bare agricultural soil

5 Rémy Fieuzal <sup>1,\*</sup> and Frédéric Baup <sup>2</sup>

6 Published: date

7 Academic Editor: name

8 <sup>1</sup> Centre d'Études de la BIOSphère (CESBIO), Université de Toulouse, CNES/CNRS/INRAe/IRD/UPS,  
9 Toulouse, France; frederic.baup@cesbio.cnes.fr

10 \* Correspondence: remy.fieuzal@cesbio.cnes.fr; Tel.: +xx-xxx-xxx-xxxx

11 **Abstract:** This paper aims at addressing the potential of polarimetric indices derived from C-band  
12 Radarsat-2 images to estimate the surface soil moisture (SSM) over bare agricultural soils. Images  
13 have been acquired during the Multispectral Crop Monitoring (MCM) experiment throughout an  
14 agricultural season over a study site located in southwestern France. Synchronously with the  
15 acquisitions of the 22 SAR images, field measurements of soil descriptors were collected on surface  
16 states with contrasting conditions, with SSM levels ranging from 2.4 to 35.3% m<sup>3</sup>·m<sup>-3</sup>, surface  
17 roughness characterized by standard deviation of roughness heights ranging from 0.5 to 7.9 cm,  
18 and soil texture showing fractions of clay, silt and sand between 9-58%, 22-77%, and 4-53%,  
19 respectively. The dataset was used to independently train and validate a statistical algorithm  
20 (random forest), SSM being estimated using the polarimetric indices and backscatter coefficients  
21 derived from the SAR images. Among the SAR signals tested, the performance levels are very  
22 uneven, as evidenced by magnitude of correlation (R<sup>2</sup>) ranging from 0.35 to 0.67. The following  
23 polarimetric indices present the best estimates of SSM: the first, second and third elements of the  
24 diagonal (T11, T22 and T33), eigenvalues (λ<sub>1</sub>, λ<sub>2</sub>, λ<sub>3</sub> from Cloude–Pottier decomposition), Shannon  
25 entropy, Freeman double-bounce and volume scattering mechanisms, the total scattered power  
26 (SPAN), and the backscattering coefficients whatever the polarization state, with correlations  
27 greater than 0.6 and with RMSE ranged between 4.8 and 5.3% m<sup>3</sup>·m<sup>-3</sup>. These performances remain  
28 limited although they are among the best SSM estimates using C-band images, comparable to those  
29 obtained with other approaches (i.e., empirical, physical based, or model inversion).

30 **Keywords:** Surface soil moisture; bare soils; synthetic aperture radar; Radarsat-2; polarimetry;  
31 random forest.  
32

## 33 1. Introduction

34 Numerous studies based on synthetic aperture radar (SAR) imagery have demonstrated the  
35 usefulness of microwave remote sensing data for surface soil moisture (SSM) estimation. Among the  
36 parameters that can be derived from these images, backscatter coefficients have been the subject of  
37 most studies especially in C-band [1-3]. The continuity of satellite missions in this frequency since  
38 the 1990s (with ERS-1/2, Envisat, Radarsat-1/2 or Sentinel-1a/b) explains the numerous studies,  
39 compared to the work carried out with other antenna configurations. In the majority of cases, the  
40 images delivered by these missions were characterized by one or even two polarization states. With  
41 missions such as Radarsat-2 and in particular the acquisition beam modes giving access to the four  
42 polarization states, the study of other metrics derived from satellite images became possible.  
43 Nevertheless, the performance and limitations associated with polarimetric approaches remain to be

44 established, as only a few studies have been carried out on the contribution of these data to the  
 45 estimation of SSM.

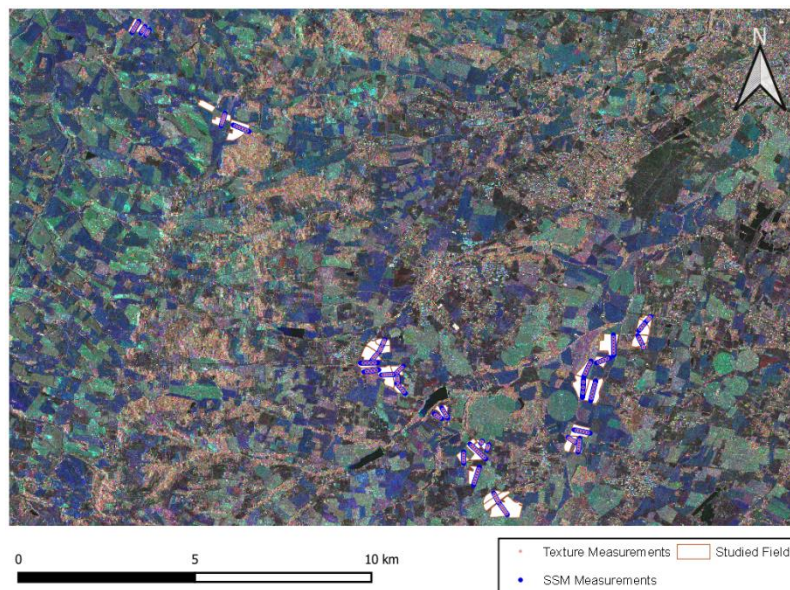
46 During the bare soil period, the sensitivity of certain polarimetric indices (i.e., alpha angle,  
 47 entropy, anisotropy) was analyzed as a function of SSM or surface roughness. Some of the tested  
 48 indices showed a low dynamic range with respect to the measured variables, the radar signals being  
 49 generally characterized by a wide dispersion [4-5]. This trend was confirmed by the work aimed at  
 50 estimating SSM in arid context, the polarimetric indices showing limited levels of performance in  
 51 retrieving the small variation intervals of measured SSM [6]. During vegetative periods, attempts to  
 52 estimate SSM were also tested on the basis of L-band data [7-9], also showing limitations in the use  
 53 of polarimetric indices.

54 In this context, the objective of this study is to address and compare the performance of  
 55 polarimetric SAR indices for SSM estimates using a statistical algorithm (i.e., random forests). The  
 56 mean features of the study site are described together with the three key soil variables collected at  
 57 each satellite overpass (sections 2.1 and 2.2 ). After images processing, independent statistical  
 58 algorithm are trained and validated for each parameter derived from the Radarsat-2 images  
 59 (procedure described in section 2.3). The performance associated with the co- and cross-polarized  
 60 backscattering coefficients, as well as those for polarimetric indices are presented, compared and  
 61 discussed in sections 3 and 4.

## 62 2. Experiments

### 63 2.1. Study site

64 From February to November 2010, the Multispectral Crop Monitoring campaign (MCM'10  
 65 campaign, see [10] for more details) was conducted on a network of agricultural plots located in  
 66 southwestern France (Figure 1). Subject to a temperate climate, the surfaces were mainly allocated to  
 67 seasonal crops (i.e., straw cereals, sunflower, corn, rapeseed, sorghum or soybean) being cultivated  
 68 on more than half of the landscape. The bare soil conditions were observed after the harvest and  
 69 before the sowing of the next crop (i.e., in spring and autumn). Several tillage events might occur on  
 70 the same plot, resulting in contrasted roughness levels (ranging from smooth before the crop sowing  
 71 to very rough after deep ploughing).



72

73 **Figure 1.** Location of the study site in southwestern France. The network of the surveyed fields is  
 74 highlighted in white and superimposed on a color-composed Radarsat-2 image acquired the  
 75 04/15/2010 (polarizations VH, VV and HH are presented in red, green and blue, respectively).

## 76 2.2. Materials

## 77 2.2.1. In situ data

## 78 • Surface soil moisture

79 The regular measurements of SSM were collected by using portable probes (ML2x from  
80 ThetaProbe), allowing to sample the top soil layer (0-5 cm) along geo-located transects. The probes  
81 delivered a signal in mV that was converted in volumetric moisture expressed in cubic meter of  
82 water per cubic meter of soil ( $\text{m}^3\cdot\text{m}^{-3}$ ), through the determination of a calibration relationship [10].  
83 The measurements were performed quasi-synchronously with satellite acquisitions over a wide  
84 range of conditions. The average values observed on the monitored plots varied between a  
85 minimum of 3.8%  $\text{m}^3\cdot\text{m}^{-3}$  and a maximum of 29.8%  $\text{m}^3\cdot\text{m}^{-3}$ , extremes observed during  
86 summer months (after the harvest of the winter crops) or during the rainy period in February and  
87 May.

## 88 • Soil texture

89 The fractions of clay, silt and sand were derived from core samples collected on the monitored  
90 plots (along the same transects used for the measurements of SSM). For each geo-located  
91 measurement, 16 core samples within a circle of 15 meters of diameter and a depth of 25 cm were  
92 performed. The monitored plots presented an interesting variability regarding soil texture, fractions  
93 being between 9-58% for the clay, between 22 and 77% for the silt and between 4 and 53% for the  
94 sand.

## 95 • Surface roughness

96 A two-meter long needle prolimeter was used to measure the micro-relief of the after each  
97 change of surface condition. Two profiles were collected parallel and perpendicular to the tillage  
98 direction of the plot, and associated to obtain 4-m-long profiles. The surface roughness was finally  
99 characterized through the derivation of two variables: the root mean square height ( $h_{\text{rms}}$ ) and  
100 correlation length ( $l_c$ ). The values of  $h_{\text{rms}}$  and  $l_c$  were derived from parallel and perpendicular profiles  
101 on ploughed, stubble disked, harrowed, prepared cloddy, prepared smooth soil. The highest values  
102 of  $h_{\text{rms}}$  were observed on the ploughed plots in the perpendicular direction (reaching a maximum of  
103 7.9 cm), while the lowest values were observed on the prepared plots in the parallel direction (with a  
104 minimum of 0.5 cm).

## 105 2.2.2. Radarsat-2 satellite data

106 Throughout the agricultural season, 22 microwave satellite images were acquired by the  
107 Canadian satellite Radarsat-2, on plots presenting bare soil conditions (Table 1). The SAR images  
108 were acquired in the C-band ( $f = 5.405$  GHz,  $\lambda = 5.5$  cm) using the full quad-polarization mode  
109 (FineQuad-Pol), which delivers products with HH, VV, HV, and VH polarizations [11]. They were  
110 acquired with eight different incidence angles, ranging from  $24^\circ$  to  $41^\circ$ , with pixel spacing of  $\sim 5$  m.

111 **Table 1.** Mean features of the Radarsat-2 acquisitions.

Mode	Acquisition Date (MM/DD)	Pass	Incidence Angle ( $^\circ$ )	Pixel size (m)
FQ5	03/05 ; 11/24	A	23.3 - 25.3	4.7x4.9
FQ6	10/21 ; 11/14	D	24.6 - 26.5	4.7x4.7
FQ10	02/26 ; 04/15 ; 05/09 ; 09/30	A	29.1 - 30.9	4.7x5.1
FQ11	03/26 ; 08/17	D	30.2 - 32.0	4.7x5.5
FQ15	03/15 ; 04/08 ; 05/02 ; 08/30 ; 10/17	A	34.3 - 36.0	4.7x4.8
FQ16	05/20 ; 07/31 ; 10/11	D	35.4 - 37.0	4.7x5.1

FQ20	11/03	A	39.1 - 40.7	4.7x4.8
FQ21	02/20 ; 03/16 ; 07/14	D	40.1 - 41.6	4.7x5.1

## 112 2.3. Method

### 113 2.3.1. Images processing

114 A radiometric calibration was first applied to the SAR images, they were then geo-coded (to  
115 correct the topographic deformations) and projected, procedures allowing the extraction of the  
116 backscattering coefficients at the plot spatial scale.

117 The processing steps aiming at deriving the polarimetric indices were performed on the SLC  
118 Radarsat-2 images, using the PolSARpro v5.0 software (Polarimetric SAR Data Processing and  
119 Educational Toolbox) [12]. Finally, the following 17 polarimetric indicators were analyzed here:  
120 entropy, anisotropy, alpha angle, and eigenvalues ( $\lambda_1$ ,  $\lambda_2$ ,  $\lambda_3$ ) (Cloude–Pottier decomposition),  
121 double-bounce, volume, and surface scattering (Freeman–Durden decomposition), SE, SE<sub>i</sub>, SE<sub>p</sub>,  
122 SPAN, RVI, and T11, T22, and T33.

### 123 2.3.2. From satellite signals to SSM estimates

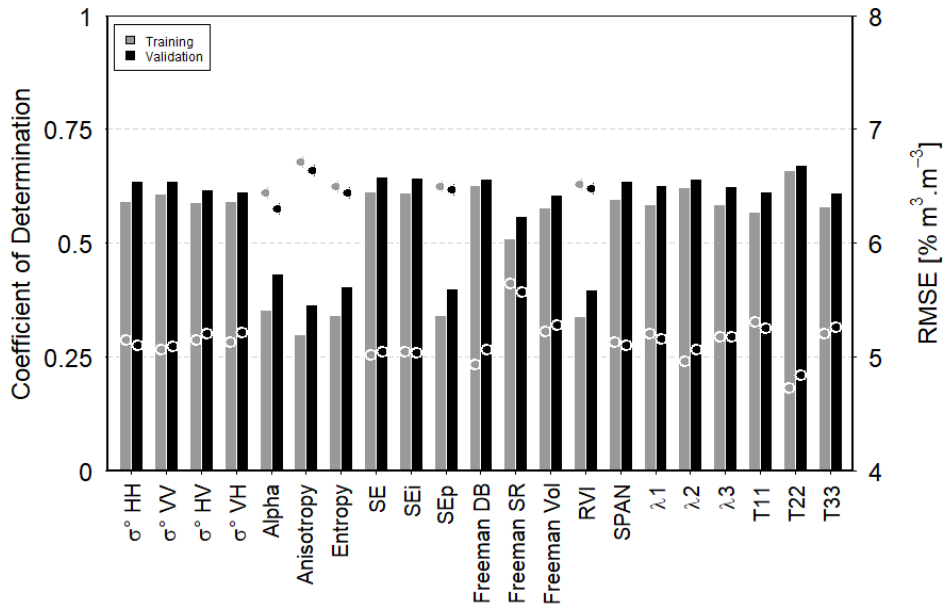
124 The parameters derived from the Radarsat-2 images (i.e., backscattering coefficients or  
125 polarimetric indices) were used independently to estimate the SSM, constituting one of the  
126 explanatory variables of the statistical algorithm proposed by [13]. In addition to the radar signals,  
127 the following variables were also considered as inputs: the incidence angles of the SAR images, the  
128 fractions of clay and sand, and the root mean square height ( $h_{rms}$ ) and correlation length ( $l_c$ )  
129 (measured in the parallel and perpendicular directions). The random forest shows satisfactory  
130 results, especially for modelling non-linear relationships. Such dynamics are a characteristic of the  
131 sensitivity of SAR signals to surface parameters observed in different studies [14-15]. In a context of  
132 estimation of backscatter coefficients, the statistical algorithm offers for example better performances  
133 than electromagnetic modelling [16-17]. The targeted variable (i.e., SSM in the present case) was  
134 derived from a weighted mean of an ensemble of estimations, obtained from independent decision  
135 trees trained on different set of samples (limiting the problems of over-adjustment or the noise  
136 influence on data).

137 Whatever the considered parameter derived from the Radarsat-2 images, an independent  
138 statistical algorithm was trained and validated on a randomly partitioned subset of the initial dataset  
139 (each subset of data containing half of the collected points). This procedure was repeated ten times.  
140 Finally, the average values of the coefficient of determination ( $R^2$ ) and the root mean square error  
141 (RMSE) were derived from the comparison between the observed and estimated values of the SSM.

## 142 3. Results

### 143 3.1. Comparison of statistical performances obtained using parameters derived from SAR images

144 An overview of the statistical performance is presented in Figure 2, summarizing the  $R^2$  and  
145 RMSE values obtained by comparing the SSM ground measurements to the estimates. The statistical  
146 approach is used with one of the parameters derived from the satellite, allowing to compare the  
147 results associated with each of the signals. A large disparity in performance levels is observed, with  
148  $R^2$  values varying between 0.30 and 0.67 and errors ranging from 4.73 to 6.71%  $m^3 \cdot m^{-3}$ . Among the  
149 best-performing parameters, estimates based on backscatter coefficients regardless of the  
150 polarization state show correlations greater than 0.60, as do the following polarimetric indicators:  
151 the first, second and third elements of the diagonal (T11, T22 and T33), eigenvalues ( $\lambda_1$ ,  $\lambda_2$ ,  $\lambda_3$  from  
152 Cloude–Pottier decomposition), Shannon entropy, Freeman double-bounce and volume scattering  
153 mechanisms, the total scattered power (SPAN). For these parameters derived from full-polarization  
154 images, the error level is between 4.8 and 5.3%  $m^3 \cdot m^{-3}$ .

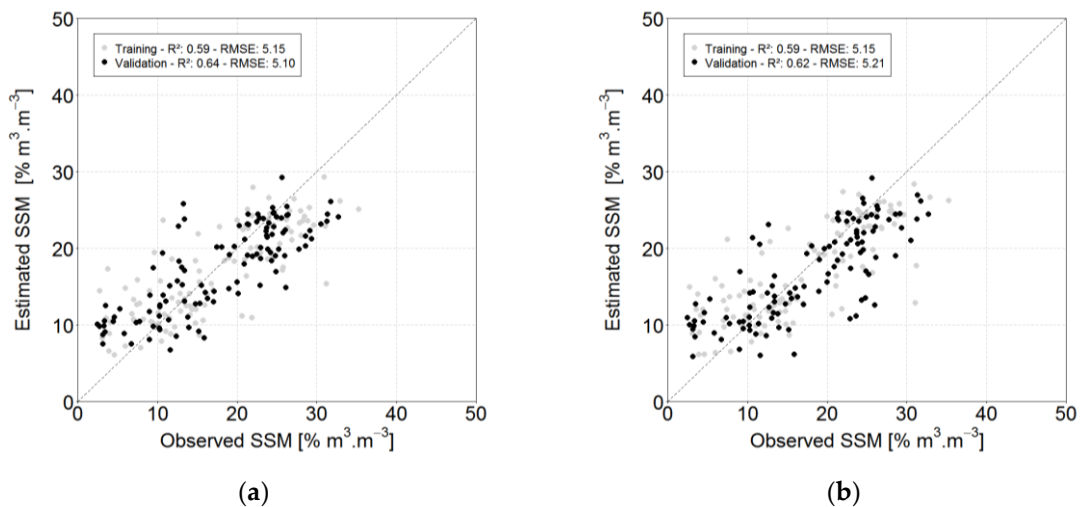


155

156 **Figure 2.** Summarize of the statistical performances (coefficients of correlation and root mean square  
 157 errors, bars and dots respectively) for the parameters derived from the Radarsat-2 images, for the  
 158 training (grey) or validation (black) subsets of samples.

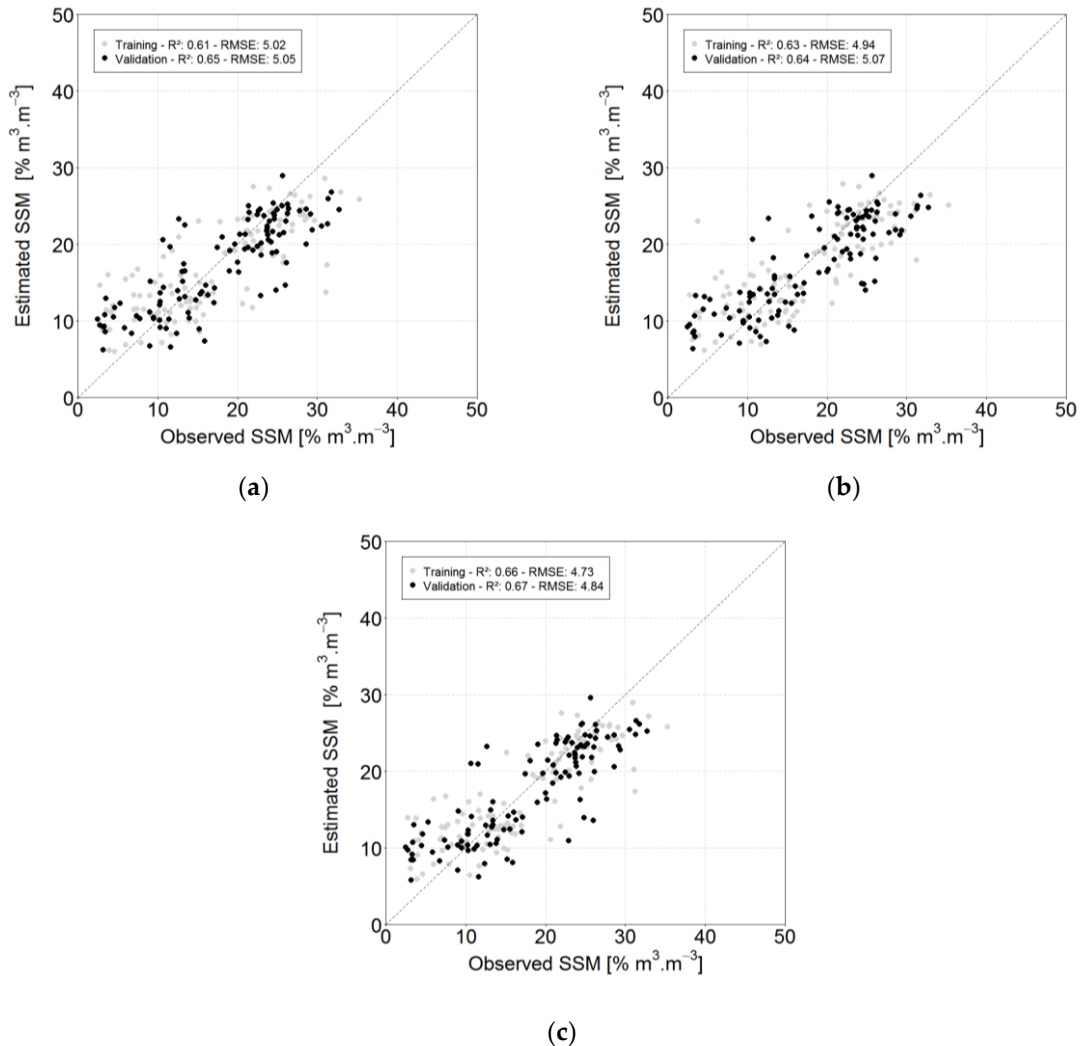
159 *3.2. Focus on promising parameters derived from the C-band images*

160 After the performance overview presented in the previous section, this section focuses on the  
 161 best results. First of all, the comparison between in situ measurements of SSM and estimates based  
 162 on backscatter coefficients, the Figure 3 showing the independent subsets of samples used during  
 163 the training and validation steps (in grey and black, respectively). In these cases, SSM estimates  
 164 based on signals acquired with HH or VV co-polarizations states are close (only results based on HH  
 165 polarization state are presented hereinafter), with  $R^2$  and RMSE close to 0.64 and 5.10%  $m^3 \cdot m^{-3}$ ,  
 166 respectively. These performance are slightly higher than the values associated with cross-polarized  
 167 signals (only HV presented hereinafter), with an  $R^2$  of 0.62 and an RMSE of 5.21%  $m^3 \cdot m^{-3}$ . These  
 168 satellite signals have already been used to estimate SSM in previous studies [1-3], thus providing a  
 169 useful baseline level of precision for comparing results obtained with polarimetric indicators.



170 **Figure 3.** Comparison between the values of observed and estimated surface soil moisture, using the  
 171 backscattering coefficients acquired in the C-band with polarization states HH (a) and HV (c). The  
 172 grey and black dots represent the estimations performed considering the training or validation  
 173 subsets of samples, respectively.

174 Among the tested parameters, only 3 cases are finally presented on Figure 4, with estimates  
 175 based on the following polarimetric indicators: Shannon entropy, Freeman double-bounce and T22  
 176 (Figures 4a, b and c, respectively). Whatever the considered parameter, the magnitude of  
 177 performance obtained with one of these signals exceeds the reference level previously established  
 178 using the backscattering coefficients, with  $R^2$  greater than 0.641 and errors less than 5.07%  $\text{m}^3\cdot\text{m}^{-3}$ . In  
 179 the end, estimates based on T22 present the best performance level for the estimation of surface  
 180 moisture at parcel scale based on microwave data acquired in C-band, with a correlation level of  
 181 0.671 and an error of 4.84%  $\text{m}^3\cdot\text{m}^{-3}$ .



182

183

184 **Figure 4.** Comparison between the values of observed and estimated surface soil moisture, using the  
 185 following polarimetric indicators: Shannon entropy (a), Freeman double-bounce (b) and T22 (c)  
 186 derived from Radarsat-2 images. The grey or black colors represent the estimations performed  
 187 considering the training or validation subsets of samples, respectively.

188 **4. Discussion**

189 Comparisons between measured and estimated SSM values show some dispersion, regardless  
 190 of the considered radar signal. In the case of estimates based on backscattering coefficients, previous  
 191 studies carried out in various contexts (i.e., on study sites with contrasting agricultural practices)  
 192 and with different methods (i.e., through empirical or modelling approaches) show a wide range of  
 193 performance levels [1-3]. The values of the statistical parameters associated with the signals acquired  
 194 in co- or cross-polarization obtained here, are in the range of the best results presented in these  
 195 studies with  $R^2$  varying between 0.61 and 0.84, and errors between 3.14 and 8.80%  $\text{m}^3\cdot\text{m}^{-3}$ .

196 Regarding estimates based on polarimetric indices, the best results are in the same performance  
 197 range as those based on backscattering coefficients. This comparison of performance over bare soil  
 198 conditions is a novelty, the results obtained so far showed very limited performance of these satellite  
 199 signals (with correlation levels ( $r$ ) not exceeding 0.50, certainly explained by the range of variation of  
 200 surface humidity values [6]) or a very low sensitivity to surface humidity [4-5]. In the end, this  
 201 assessment is a necessary preliminary step for the use of these signals for the estimation of SSM  
 202 during the vegetation period, the first studies having shown for the moment very limited results  
 203 [7-9].

## 204 5. Conclusions

205 This study presents a comparison of the performance of a set of parameters that can be derived  
 206 from radar images acquired with the four polarization states on the same study site (showing  
 207 important variations of the surface parameters). The results are established on the basis of a  
 208 statistical approach, implemented independently for each of the considered satellite signals, and  
 209 allowing to classify the levels of accuracy of the polarimetric indices and backscattering coefficients.  
 210 Among the best results, Shannon entropy, Freeman double-bounce and T22 show performances  
 211 equivalent or even superior to those obtained with the backscattering coefficients.

212 The analysis presented in this study are a first step in the perspective that would lead to  
 213 propose a new approach to estimate SSM. The next step would be to determine the combination of  
 214 polarimetric indices allowing a monitoring of SSM, without recourse to exogenous data, whether on  
 215 the level of roughness or texture.

216 **Acknowledgments:** Authors would like to thank especially Space Agencies for their support and confidence  
 217 they have in this project (CNES, ESA, and DLR). Many thanks to farmers and people who helped for collecting  
 218 ground data.

219 **Author Contributions:** The authors contributed equally to the various steps required to complete this study.  
 220 All authors have read and agreed to the published version of the manuscript.

221 **Conflicts of Interest:** The authors declare no conflict of interest.

## 222 References

- 223 1. Zribi, M.; Le Hégarat-Masclé, S.; Ottlé, C.; Kammoun, B.; Guerin, C. Surface soil moisture estimation from  
 224 the synergistic use of the (multi-incidence and multi-resolution) active microwave ERS Wind  
 225 Scatterometer and SAR data. *Remote Sens. Environ.* **2003**, *86*, 30–41.
- 226 2. Fieuzal, R.; Duchemin, B.; Jarlan, L.; Zribi, M.; Baup, F.; Merlin, O.; Hagolle, O.; Garatuza-Payan, J.  
 227 Combined use of optical and radar satellite data for the monitoring of irrigation and soil moisture of wheat  
 228 crops. *Hydrol. Earth Syst. Sci.* **2011**, *15*, 1117–1129.
- 229 3. Gherboudj, I.; Magagi, R.; Berg, A.A.; Toth, B. Soil moisture retrieval over agricultural fields from  
 230 multi-polarized and multi-angular RADARSAT-2 SAR data. *Remote Sens. Environ.* **2011**, *115*, 33–43.
- 231 4. Baghdadi, N.; Cresson, R.; Pottier, E.; Aubert, M.; Zribi, M.; Jacome, A.; Benabdallah, S. A potential use for  
 232 the C-band polarimetric SAR parameters to characterize the soil surface over bare agriculture fields. *IEEE*  
 233 *Trans. Geosci. Remote Sens.* **2012**, *50*, 3844–3858.
- 234 5. Baghdadi, N.; Dubois-Fernandez, P.; Dupuis, X.; Zribi, M. Sensitivity of main polarimetric parameters of  
 235 multifrequency polarimetric SAR data to soil moisture and surface roughness over bare agricultural soils.  
 236 *IEEE Geosci. Remote Sens. Lett.* **2013**, *10*, 731–735.
- 237 6. Yang, L.; Feng, X.; Liu, F.; Liu, J.; Sun, X. Potential of soil moisture estimation using C-band polarimetric  
 238 SAR data in arid regions. *Inter. Journal of Remote Sens.* **2019**, *40*, 2138–2150.
- 239 7. Hajnsek, I.; Jagdhuber, T.; Schon, H.; Papathanassiou, K.P. Potential of estimating soil moisture under  
 240 vegetation cover by means of PolSAR. *IEEE Trans. Geosci. Remote Sens.* **2009**, *47*, 442–454.
- 241 8. Wang, H.; Magagi, R.; Goita, K.; Jagdhuber, T.; Hajnsek, I. Evaluation of simplified polarimetric  
 242 decomposition for soil moisture retrieval over vegetated agricultural fields. *Remote Sens.* **2016**, *8*, 142.
- 243 9. Wang, H.; Magagi, R.; Goita, K. Comparison of different polarimetric decompositions for soil moisture  
 244 retrieval over vegetation covered agricultural area. *Remote Sens. Environ.* **2017**, *199*, 120–136.

- 245 10. Baup, F.; Fieuzal, R.; Marais-Sicre, C.; Dejoux, J.-F.; le Dantec, V.; Mordelet, P.; Claverie, M.; Hagolle, O.;  
246 Lopes, A.; Keravec, P.; Ceschia, E.; Mialon, A.; Kidd, R. MCM'10: An experiment for satellite multi-sensors  
247 crop monitoring from high to low resolution observations. *2012 IEEE International Geoscience and Remote*  
248 *Sensing Symposium*, Munich, **2012**, 4849-4852.
- 249 11. Morena, L.C.; James, K.V.; Beck, J. An introduction to the RADARSAT-2 mission. *Can. J. Remote Sens.* **2004**,  
250 30(3), 221-234.
- 251 12. Pottier, E.; Ferro-Famil, L. PolSARPro V5.0: An ESA educational toolbox used for self-education in the  
252 field of POLSAR and POL-INSAR data analysis. *2012 IEEE International Geoscience and Remote Sensing*  
253 *Symposium*, Munich, **2012**, 7377-7380
- 254 13. Breiman, L. Random Forests. *Machine Learning*, **2001**, 45(1), 5-32.
- 255 14. Ulaby, F.T.; Batlivala, P.P.; Dobson, M.C. Microwave backscatter dependence on surface roughness, soil  
256 moisture, and soil texture: Part I-Bare Soil", *IEEE Trans. Geosci. Electronics.* **1978**, 16(4), 286-295.
- 257 15. Hallikainen, M.T.; Ulaby, F.T.; Dobson, M.C.; El-Rayes, M.A.; Lil-Kun, W. Microwave dielectric behavior  
258 of wet soil—Part 1: Empirical models and experimental observations. *IEEE Trans. Geosci. Remote Sens.* **1985**,  
259 23, 25-34.
- 260 16. Fieuzal, R.; Baup, F. Improvement of bare soil semiempirical radar backscattering models (Oh and Dubois)  
261 with SAR multi-spectral satellite data (at X, C and L bands). *Advances in Remote Sens.*, **2016**, 5(4), 296-314,  
262 2016.
- 263 17. Fieuzal, R.; Baup, F. Statistical estimation of backscattering coefficients in X-band over bare agricultural  
264 aoiils," *2020 Mediterranean and Middle-East Geoscience and Remote Sensing Symposium (M2GARSS)*, Tunis,  
265 Tunisia, **2020**, 302-305.



© 2020 by the authors; licensee MDPI, Basel, Switzerland. This article is an open access article distributed under the terms and conditions of the Creative Commons by Attribution (CC-BY) license (<http://creativecommons.org/licenses/by/4.0/>).